97. *N* and Δ Resonances

Revised February 2018 by V. Burkert (Jefferson Lab), E. Klempt (University of Bonn), U. Thoma (University of Bonn), L. Tiator (University of Mainz), and R.L. Workman (George Washington University).

97.1. Introduction

The excited states of the nucleon have been studied in a large number of formation and production experiments. Until recently, the Breit-Wigner masses and widths, the pole positions, and the elasticities of the N and Δ resonances in the Baryon Summary Table came largely from partial-wave analyses of πN total, elastic, and charge-exchange scattering data. The most comprehensive analyses were carried out by the Karlsruhe-Helsinki (KH80) [1], Carnegie Mellon-Berkeley (CMB80) [2], and George Washington U (GWU) [3] groups. Partial-wave analyses have also been performed on much smaller πN reaction data sets to get ηN, $K\Lambda$, and $K\Sigma$ branching fractions (see the Listings for references). Other branching fractions come from analyses of $\pi N \to \pi\pi N$ data.

In recent years, a large amount of data on photoproduction of many final states has been accumulated, and these data are beginning to tell us much about the properties of baryon resonances. A survey of data on photoproduction can be found in the proceedings of recent conferences [4] and workshops [5], and in recent reviews [6,7].

97.2. Naming scheme for baryon resonances

In the past, when nearly all resonance information came from elastic πN scattering, it was common to label resonances with the incoming partial wave $L_{2I,2J}$, as in $\Delta(1232)P_{33}$ and $N(1680)F_{15}$. However, most recent information has come from γN experiments. Therefore, we have replaced $L_{2I,2J}$ with the spin-parity J^P of the state, as in $\Delta(1232)3/2^+$ and $N(1680)5/2^+$; this name gives intrinsic properties of the resonance that are independent of the specific particles and reactions used to study them. This applies equally to all baryons, including Ξ resonances and charm baryons that are not produced in formation experiments. We do not, however, attach the mass or spin-parity to the names of the ground-state ("stable") baryons $N, \Lambda, \Sigma, \Xi, \Omega, \Lambda_c, \cdots$.

97.3. Using the *N* and Δ listings

Tables 97.1 and 97.2 list all the N and Δ entries in the Baryon Listings and give our evaluation of the overall status and the status channel by channel. Only the established resonances (overall status 3 or 4 stars) are promoted to the Baryon Summary Table. We long ago omitted from the Listings information from old analyses, prior to KH80 and CMB80, which can be found in earlier editions. A rather complete survey of older results was given in our 1982 edition [8].

As a rule, we award an overall status **** or *** only to those resonances which are derived from analyses of data sets that include precision differential cross sections and polarization observables, and are confirmed by independent analyses. All other signals are given ** or * status. New results that are not accompanied by proper error evaluation are

less valuable for evaluating star ratings. The following criteria are guidelines for future error analysis.

1. Uncertainties in resonance parameters: The publication should have a detailed discussion on how the uncertainties of parameters were estimated. This requires that the error estimates go beyond the simple fit error as e.g. given by MINUIT, and the robustness of the results should be demonstrated.

2. Fit quality: Concrete measures for the fit quality should be provided. The reduced global χ^2 value of the fit, while useful, is insufficient. Other possibilities include quoting variations of local χ^2 values in kinematic regions where evidence for new resonances, or significantly improved information on resonance parameters, is claimed.

3. Weight factors in observables: Analyses sometimes use weight factors for certain data sets to either increase or reduce their impact on the results. This has been particularly important when polarization observables are involved, which often are sensitive to resonance amplitudes through interferences, but usually have much poorer statistics than differential cross section data. To evaluate sensitivities, the resulting resonance parameters should be checked against variations of the specific weight factors.

Claims of evidence for new baryon states must be based on a sufficiently complete set of partial waves in the fit. The robustness of signals must be demonstrated, e.g. by examining the effect of higher partial waves in the fit.

97.4. Properties of resonances

Resonances are defined by poles of the S-matrix, whether in scattering, production or decay matrix elements. These are poles in the complex plane in s, as discussed in the new review on *Resonances*. As is traditional, we quote here the pole positions in the complex energy $w = \sqrt{s}$ plane. Crucially, the position of the pole of the S-matrix is independent of the process, and the production and decay properties factorize. This is the rationale for listing the pole position first for each resonance.

These key properties of the S-matrix pole are in contrast to other quantities related to resonance phenomena, such as Breit-Wigner parameters or any K-matrix pole. Thus, Breit-Wigner parameters depend on the formalism used, such as angular-momentum barrier factors, or cut-off parameters, and the assumed or modeled background. However, the accurate determination of pole parameters from the analysis of data on the real energy axis is not necessarily simple or even straightforward. It requires the implementation of the correct analytic structure of the relevant (often coupled) channels. The example in the meson sector of the σ-pole highlights the need to incorporate right and left hand cut analyticity (and their relation imposed by crossing symmetry) into a dispersive analysis to obtain a robust determination of the pole position for a very short-lived state close to the lowest threshold. The development of general methods that are simpler to implement in the baryon sector is a research problem of current interest, often exploiting techniques introduced long ago when the experimental data were far poorer than those presently available for reactions like $\gamma N \to \pi N$ [9]. No consensus yet exists for the use of any particular method, beyond the need to incorporate the general properties mentioned here and discussed more fully in the review of *Resonances*.

Table 97.1. The status of the N resonances and their decays. Sub-threshold decay modes are omitted. Only resonances with an overall status of ∗∗∗ or ∗∗∗∗ are included in the main Baryon Summary Table.

			Status as seen in									
Particle	J^P	overall	$N\gamma$	$N\pi$	$\Delta\pi$	$N\sigma$	$N\eta$	ΛK	ΣK	$N\rho$	$N\omega$	$N\eta'$
N	$1/2^+$	****										
$N(1440)$	$1/2^+$	****	****	****	****	***						
$N(1520)$	$3/2^-$	****	****	****	****	**	****					
$N(1535)$	$1/2^-$	****	****	****	***	*	****					
$N(1650)$	$1/2^-$	****	****	****	***	*	****	*				
$N(1675)$	$5/2^-$	****	****	****	****	***	*	*	*			
$N(1680)$	$5/2^+$	****	****	****	****	***	*	*	*			
$N(1700)$	$3/2^-$	***	**	***	***	*	*			*		
$N(1710)$	$1/2^+$	****	****	****	*		***	**	*	*	*	
$N(1720)$	$3/2^+$	****	****	****	***	*	*	****	*	*	*	
$N(1860)$	$5/2^+$	**	*	**		*	*					
$N(1875)$	$3/2^-$	***	**	**	*	**	*	*	*	*	*	
$N(1880)$	$1/2^+$	***	**	*	**	*	*	**	**		**	
$N(1895)$	$1/2^-$	****	****	*	*	*	****	**	**	*	*	****
$N(1900)$	$3/2^+$	****	****	**	**	*	*	**	**		*	**
$N(1990)$	$7/2^+$	**	**	**			*	*	*			
$N(2000)$	$5/2^+$	**	**	*	**	*	*				*	
$N(2040)$	$3/2^+$	*		*								
$N(2060)$	$5/2^-$	***	***	**	*	*	*	*	*	*	*	
$N(2100)$	$1/2^+$	***	**	***	**	**	*	*		*	*	**
$N(2120)$	$3/2^-$	***	***	**	**	**		**	*		*	*
$N(2190)$	$7/2^-$	****	****	****	****	**	*	**	*	*	*	
$N(2220)$	$9/2^+$	****	**	****			*	*	*			
$N(2250)$	$9/2^-$	****	**	****			*	*	*			
$N(2300)$	$1/2^+$	**		**								
$N(2570)$	$5/2^-$	**		**								
$N(2600)$	$11/2^-$	***		***								
$N(2700)$	$13/2^+$	**		**								

****	Existence is certain.
***	Existence is very likely.
**	Evidence of existence is fair.
*	Evidence of existence is poor.

Table 97.2. The status of the Δ resonances and their decays. Sub-threshold decay modes are omitted. Only resonances with an overall status of *** or **** are included in the main Baryon Summary Table.

			Status as seen in					
Particle	J^P	overall	$N\gamma$	$N\pi$	$\Delta\pi$	ΣK	$N\rho$	$\Delta\eta$
Δ(1232)	$3/2^+$	****	****	****				
Δ(1600)	$3/2^+$	****	****	***	****			
Δ(1620)	$1/2^-$	****	****	****	****			
Δ(1700)	$3/2^-$	****	****	****	****	*	*	
Δ(1750)	$1/2^+$	*	*	*		*		
Δ(1900)	$1/2^-$	***	***	***	*	**	*	
Δ(1905)	$5/2^+$	****	****	****	**	*	*	**
Δ(1910)	$1/2^+$	****	***	****	**	**		*
Δ(1920)	$3/2^+$	***	***	***	***	**		**
Δ(1930)	$5/2^-$	***	*	***	*	*		
Δ(1940)	$3/2^-$	**	*	**	*			*
Δ(1950)	$7/2^+$	****	****	****	**	***		
Δ(2000)	$5/2^+$	**	*	**	*		*	
Δ(2150)	$1/2^-$	*		*				
Δ(2200)	$7/2^-$	***	***	**	***	**		
Δ(2300)	$9/2^+$	**		**				
Δ(2350)	$5/2^-$	*		*				
Δ(2390)	$7/2^+$	*		*				
Δ(2400)	$9/2^-$	**	**	**				
Δ(2420)	$11/2^+$	****	*	****				
Δ(2750)	$13/2^-$	**		**				
Δ(2950)	$15/2^+$	**		**				

****	Existence is certain.
***	Existence is very likely.
**	Evidence of existence is fair.
*	Evidence of existence is poor.

97.5. Photoproduction

A new approach to the nucleon excitation spectrum is provided by dedicated facilities at the Universities of Bonn, Grenoble, and Mainz, and at the national laboratories Jefferson Lab in the US and SPring-8 in Japan. High-precision cross sections and polarization observables for the photoproduction of pseudoscalar mesons provide a data set that is approaching a "complete experiment," one that fully constrains the four complex amplitudes describing the spin-structure of the reaction [11]. A large number of photoproduction reactions has been studied.

In pseudoscalar meson photoproduction, the four independent helicity amplitudes can be expressed in terms of the four CGLN [12] amplitudes allowed by Lorentz and gauge invariance. These amplitudes can be expanded in a series of electric and magnetic multipoles. Except for $J = 1/2$, one electric and one magnetic multipole contributes to each J^P combination.

For a given state, these two amplitudes determine the resonance photo-decay helicity amplitudes $A_{1/2}$ and $A_{3/2}$. As described below, this resonance extraction has been carried out either assuming a Breit-Wigner resonance or at the pole.

If a Breit-Wigner parametrization is used, the $N\gamma$ partial width, Γ_γ, is given in terms of the helicity amplitudes $A_{1/2}$ and $A_{3/2}$ by

$$\Gamma_\gamma = \frac{k_{\rm BW}^2}{\pi}\frac{2m_N}{(2J+1)m_{\rm BW}}\Big(|A_{1/2}|^2 + |A_{3/2}|^2\Big) \ . \tag{1}$$

Here m_N and $m_{\rm BW}$ are the nucleon and resonance masses, J is the resonance spin, and $k_{\rm BW}$ is the photon c.m. decay momentum. Most earlier analyses have provided these real quantities $A_{1/2}$ and $A_{3/2}$.

More recent studies have quoted related complex quantities, evaluated at the T-matrix pole. These complex helicity amplitudes, $\tilde{A}_{1/2}$ and $\tilde{A}_{3/2}$, can be cast onto the form

$$\tilde{A}_h = \sqrt{\frac{\pi(2J+1)w_{\rm pole}}{m_N k_{\rm pole}^2}}\ \frac{Res(T_h(\gamma N \to N\,b))}{\sqrt{Res(T\,(N\,b \to N\,b))}} \tag{2}$$

where the residues (Res) are evaluated at the pole position, $w_{\rm pole}$, and $k_{\rm pole}^2 = (w_{\rm pole}^2 - m_N^2)^2/4w_{\rm pole}^2$ [13]. For Breit-Wigner amplitudes, $w_{\rm pole} = m_{\rm BW}$ and $\tilde{A}_h = A_h$. Similar relations for the photo and electro couplings at the pole position can be found in [14,15].

The determination of eight real numbers from four complex amplitudes (with one overall phase undetermined) requires at least seven independent measurements. At least one further measurement is required to resolve discrete ambiguities that result from the fact that data are proportional to squared amplitudes. Photon beams and nucleon targets can be polarized (with linear or circular polarization $P_\perp$, $P_\odot$ and $\vec{T}$, respectively); the recoil polarization of the outgoing baryon $\vec{R}$ can be measured. The experiments can be divided into three classes: (1) the beam and target are polarized (BT); (2) the beam is

polarized and the recoil baryon polarization is measured (BR); (3) the target is polarized and the recoil polarization is measured (TR). Different sign conventions are used in the literature, as summarized in [16].

One of the best studied reactions is $\gamma p \to \Lambda K^+$. Published data include differential cross sections, the beam asymmetry Σ, the target asymmetry T, the recoil polarization P, and the BR double-polarization variables $C_{x'}, C_{z'}, O_{x'}$, and $O_{z'}$. For the photoproduction of pions and etas, off proton and neutron targets, differential cross sections, single- and double-polarization asymmetries have been measured, mainly for pions.

97.6. Electroproduction

Electroproduction of mesons provides information on the internal structure of resonances. The helicity amplitudes are functions of the (squared) momentum transfer $Q^2 = -(e - e')^2$, where e and e' are the 4-momenta of the incident and scattered electron, and a third amplitude, $S_{1/2}$, measures the resonance response to the longitudinal component of the virtual photon. Most data stem from the reactions $e^- p \to e^- n\pi^+$ and $e^- p \to e^- p\pi^0$ but also the reactions $e^- p \to e^- p\eta$, $e^- p \to e^- p\pi^+\pi^-$, and $e^- p \to e^- \Lambda(\Sigma^0)K^+$ have been studied. The data and their interpretation are reviewed in Refs. [18,19].

The transition to the $\Delta(1232)3/2^+$ is often quantified in terms of the magnetic dipole transition moment M_{1+} (or the magnetic transition form factor $G^*_{M,Ash}(Q^2)$) [20], and the electric and scalar quadrupole transition moments E_{1+} and S_{1+}. Figure 97.1 shows the strength of the $p \to \Delta^+$ transition plotted versus the photon virtuality Q^2. At $Q^2 = 0$, M_{1+} dominates the resonance transition strength. The two amplitudes E_{1+} and S_{1+} imply a quadrupole deformation of the transition to the lowest excited state. The magnitude of $R_{EM} = E_{1+}/M_{1+}$ remains nearly constant, while the magnitude of $R_{SM} = S_{1+}/M_{1+}$ increases rapidly up to 25% at the highest Q^2 value.

Figure 97.2 shows the transverse and scalar helicity amplitudes for the $N(1440)1/2^+$, $N(1520)3/2^-$, and $N(1535)1/2^-$ resonances from JLab [18]. Similar results have been achieved at Mainz [19]. For the states $N(1440)1/2^+$ and $N(1520)3/2^-$, helicity amplitudes and $\pi\Delta$ and ρp decays were determined at JLab in an analysis of $\pi^+\pi^- p$ electroproduction [21]. The data show distinctly different Q^2 dependencies that indicate different internal structures.

The $N(1520)3/2^-$ helicity amplitudes reveal the dominance of its three-quark nature: the $A_{3/2}$ amplitude is large at the photon point and decreases rapidly $\sim Q^{-5}$ with increasing Q^2; $A_{1/2}$ is small at the photon point, increases rapidly with Q^2 and then falls off with $\sim Q^{-3}$. Quantitative agreement with the data is, however, achieved only when meson cloud effects are included.

At high Q^2, both amplitudes for $N(1440)1/2^+$ are qualitatively described by light front quark models [22]: at short distances the resonance behaves as expected from a radial excitation of the nucleon. On the other hand, $A_{1/2}$ changes sign at about $0.6\,\mathrm{GeV}^2$. This remarkable behavior has not been observed before for any nucleon form factor or transition amplitude. Obviously, an important change in the structure occurs when the resonance is probed as a function of Q^2.

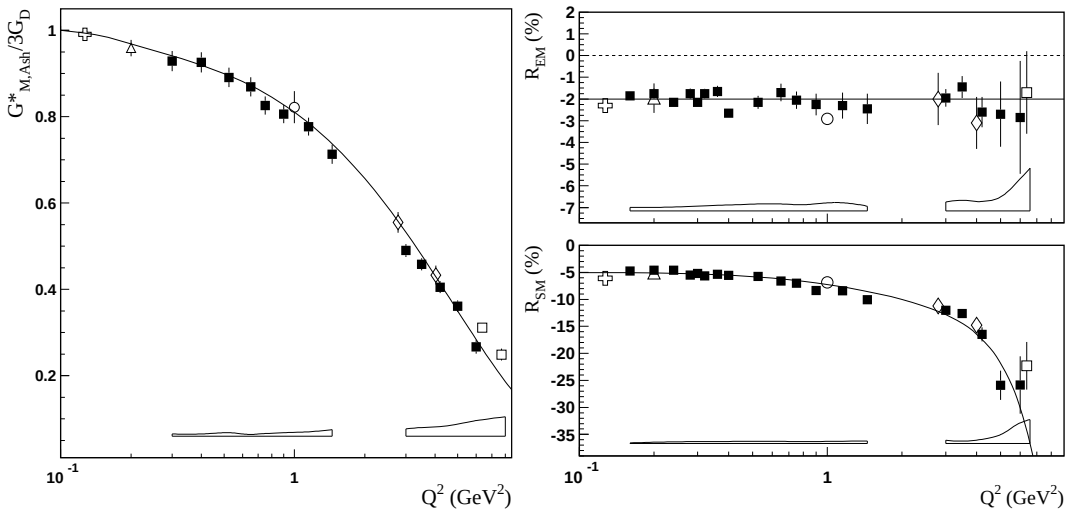

Figure 97.1: Left: The magnetic transition form factor for the $\gamma^* p \to \Delta^+(1232)$ transition versus the photon virtuality Q^2. Right: The electric and scalar quadrupole ratios R_{EM} and R_{SM}. The different symbols are results from different experiments at JLab (squares, diamonds, circle) and MAMI (triangle, cross). The boxes near the horizontal axis indicate model uncertainties of the squares. Curves to guide the eyes.

The Q^2 dependence of $A_{1/2}$ of the $N(1535)1/2^-$ resonance exhibits the expected Q^{-3} dependence, except for small Q^2 values where meson cloud effects set in.

Figure 97.3 shows the transverse and scalar amplitudes for three states in the 3rd nucleon resonance region, the $\Delta(1620)1/2^-$, the $N(1675)5/2^-$ and $N(1680)5/2^+$. The latter two states have nearly degenerate masses and are parity partners. In the quark model picture, the transverse amplitudes for $N(1675)5/2^-$ on the proton are suppressed due to the Moorhouse selection rule, allowing for a quantitative evaluation of the meson-baryon contributions. The data show significant meson-baryon strength in the $A_{1/2}$ amplitude even at quite high Q^2, while $A_{3/2}$ drops much faster with Q^2. $N(1680)5/2^+$ shows qualitatively the features predicted in constituent quark models, a dominant $A_{3/2}$ at the real photon point that drops rapidly with increasing Q^2, while $A_{1/2}$ becomes the dominant contribution at high Q^2, indicating a switch of the helicity structure in the resonance transition at short distances.

97.7. Partial wave analyses

Several PWA groups are now actively involved in the analysis of the new data. The GWU group maintains a nearly complete database covering reactions from πN and KN elastic scattering to $\gamma N \to N\pi$, $N\eta$, and $N\eta'$. It is presently the only group determining πN elastic amplitudes from scattering data in sliced energy bins. Given the high-precision of photoproduction data already or soon to be collected, the spectrum of N and Δ resonances will in the near future be better known.

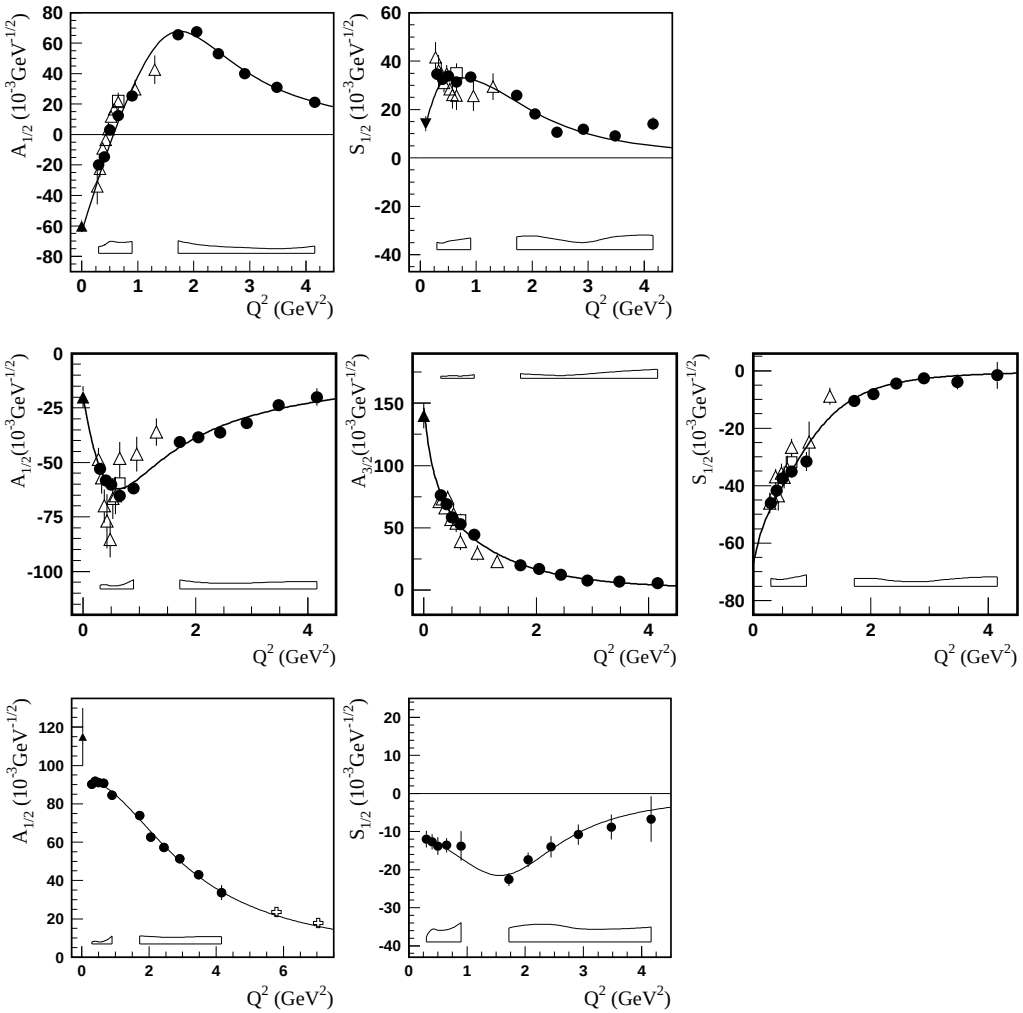

Figure 97.2: Transverse and scalar (longitudinal) helicity amplitudes for $\gamma p \to N(1440)1/2^+$ (top), $\gamma p \to N(1520)3/2^-$ (center), and $\gamma p \to N(1535)1/2^-$ (bottom) as extracted from the JLab/CLAS data in $n\pi^+$ production (full circles), MAMI/A1 data in $p\pi^0$ production (full down triangle), in $p\pi^+\pi^-$ (open triangles), and combined single and double pion production (open squares). The solid triangle is the PDG 2014 value at $Q^2 = 0$. The open boxes are the model uncertainties of the full circles.

Fits to the data are performed by various groups with the aim to understand the reaction dynamics and to identify N and Δ resonances. For practical reasons, approximations have to be made. We mention several analyses here: (1) The Mainz unitary isobar model [23] focuses on the correct treatment of the low-energy domain. Resonances are added to the unitary amplitude as a sum of Breit-Wigner amplitudes. This model also obtains resonance transition form factors and helicity amplitudes from electroproduction [19]. (2) For $N\pi$ electroproduction, the Yerevan/JLab group uses both the unitary isobar model and the dispersion relation approach developed in [22]. A

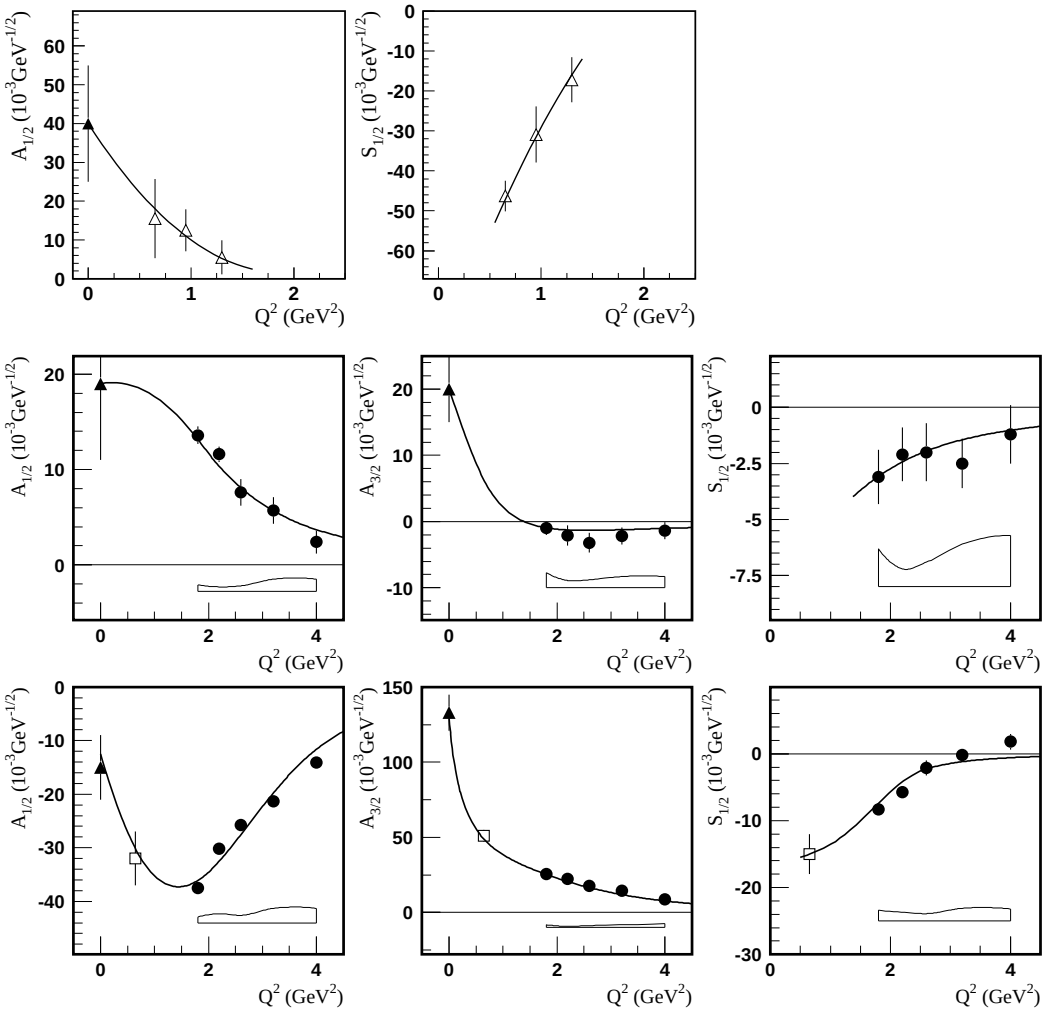

Figure 97.3: Transverse and scalar helicity amplitudes for $\gamma p \to \Delta(1620)1/2^-$ (top), $\gamma p \to N(1675)5/2^-$ (center), and $\gamma p \to N(1680)5/2^+$ (bottom) as extracted from the JLab/CLAS data in $n\pi^+$ production (full circles), $p\pi^+\pi^-$ (open triangles), combined single and double pion production (open square). The solid triangle is the 2014 PDG value at $Q^2 = 0$. The open boxes are the model uncertainties of the full circles. The curves are to guide the eye.

phenomenological model was developed to extract resonance couplings and partial decay widths from exclusive $\pi^+\pi^- p$ electroproduction [21]. (3) Multichannel analyses using K-matrix parameterizations derive background terms from a chiral Lagrangian - providing a microscopical description of the background - (Giessen [24,25]) or from phenomenology (KSU [26,27], Bonn-Gatchina [28]) . (4.) Several groups (EBAC-Jlab [29,30], ANL-Osaka [31], Dubna-Mainz-Taipeh [32], Bonn-Jülich [33,34,35], Valencia [36]) use dynamical reaction models, driven by chiral Lagrangians, which take dispersive parts of intermediate states into account. Several other groups have made important contributions. The Giessen group pioneered multichannel analyses of large data sets on

pion- and photo-induced reactions [24,25]. The Bonn-Gatchina group included recent high-statistics data and reported systematic searches for new baryon resonances in all relevant partial waves. A summary of their results can be found in [28].

References:

1. G. Höhler, Pion-Nucleon Scattering, Landolt-Börnstein Vol. I/9b2 (1983), ed. H. Schopper, Springer Verlag.
2. R.E. Cutkosky *et al.*, Baryon 1980, *IV International Conference on Baryon Resonances*, Toronto, ed. N. Isgur, p. 19.
3. R.A. Arndt *et al.*, Phys. Rev. **C74**, 045205 (2006).
4. "Hadron 2011: 14th International Conference on Hadron Spectroscopy", München, Germany, June, 13 - 17, 2011, published in eConf.
5. "NSTAR 2013: 9th International Workshop on the Physics of Excited Nucleons", 27-30 May 2013, Peñíscola, Spain.
6. E. Klempt and J.M. Richard, Rev. Mod. Phys. **82**, 1095 (2010).
7. V. Credé and W. Roberts, Rept. on Prog. in Phys. **76**, 076301 (2013).
8. M. Roos *et al.*, Phys. Lett. **B111**, 1 (1982).
9. A. Svarc *et al.*, Phys. Rev. **C88**, 035206 (2013).
10. R.H. Dalitz, R.G. Moorhouse, Proc. Royal Soc. London **A318**, 279 (1970).
11. C. G. Fasano *et al.*, Phys. Rev. **C46**, 2430 (1992).
12. G.F. Chew *et al.*, Phys. Rev. **106**, 1345 (1957).
13. R.L. Workman, L. Tiator, and A. Sarantsev, Phys. Rev. **C87**, 068201 (2013).
14. N. Suzuki, T. Sato, and T.-S.H. Lee, Phys. Rev. **C82**, 045206 (2010).
15. H. Kamano, Phys. Rev. **C88**, 045203 (2013).
16. A.M. Sandorfi *et al.*, AIP Conf. Proc. **1432**, 219 (2012).
17. R. Beck and A. Thiel, J. Phys. Conf. Ser. **295**, 012023 (2011).
18. I. G. Aznauryan and V. D. Burkert, Prog. in Part. Nucl. Phys. **67**, 1 (2012).
19. L. Tiator *et al.*, Eur. Phys. J. ST **198**, 141 (2011);
    S. Štajner *et al.*, Phys. Rev. Lett. **119**, 022001 (2017).
20. W.W. Ash, Phys. Lett. **B24**, 165 (1967).
21. V.I. Mokeev *et al.* [CLAS Collab.], Phys. Rev. **C86**, 035203 (2012).
22. I.G. Aznauryan, Phys. Rev. **C67**, 015209 (2003).
23. D. Drechsel, S.S. Kamalov, and L. Tiator, Eur. Phys. J. **A34**, 69 (2007).
24. G. Penner and U. Mosel, Phys. Rev. **C66**, 055211 (2002).
25. G. Penner and U. Mosel, Phys. Rev. **C66**, 055212 (2002).
26. D.M. Manley and E.M. Saleski, Phys. Rev. **D45**, 4002 (1992).
27. M. Shrestha and D.M. Manley, Phys. Rev. **C86**, 055203 (2012).
28. A.V. Anisovich *et al.*, Eur. Phys. J. **A48**, 15 (2012).
29. A. Matsuyama, T. Sato, and T.-S.H. Lee, Phys. Reports **439**, 193 (2007).
30. T. Sato and T.-S.H. Lee, J. Phys. **G36**, 073001 (2009).
31. H. Kamano *et al.*, Phys. Rev. **C88**, 035209 (2013).
32. G.Y. Chen *et al.*, Phys. Rev. **C76**, 035206 (2007).
33. M. Döring *et al.*, Phys. Lett. **B681**, 26 (2009).
34. M. Döring *et al.*, Nucl. Phys. **A829**, 170 (2009).
35. D. Rönchen *et al.*, Eur. Phys. J. **A49**, 44 (2013).

36. S. Sarkar, E. Oset, and M.J. Vicente Vacas, Nucl. Phys. **A750**, 294 (2005) [Erratum-ibid. **A780**, 78 (2006)].